Precoder Design for MIMO Sensing with Scatterers

Yiming Liu and Wei Yu
Department of Electrical and Computer Engineering, University of Toronto, Canada
E-mails: eceym.liu@mail.utoronto.ca, weiyu@ece.utoronto.ca

***Abstract*—This paper considers the problem of MIMO sensing precoding design for estimating the azimuth angles of multiple targets in the presence of interfering scatterers. We show that unlike the case with no scatterers, where the optimization of MIMO sensing sequence reduces to the optimization of a single transmit covariance matrix, when interfering scatterers are present, the optimization must be over the entire MIMO sensing sequence across the sensing interval. This paper proposes a methodology for designing such MIMO precoding sequences by formulating the problem as that of minimizing the Bayesian Cramér-Rao lower bound for estimating multiple target angles subject to interference from the scatterers. We show that when the path-loss coefficients of the targets and the scatterers are modeled as nuisance variables with zero mean, the problem can be cast as a max-min fractional program, which can be efficiently solved using a linear transform technique. Numerical results unveil nontrivial sweeping-like beam patterns that should be synthesized by the transmit antennas to facilitate sensing and to suppress interference.**

I. Introduction

Integrated sensing and communications (ISAC), which aims to utilize existing communications infrastructure for sensing applications, is a crucial area of research interest for future wireless communication systems. Multiple-input multiple-output (MIMO) technique is important for communications due to its ability to utilize spatial dimensions to improve spectral efficiency and to suppress interference. In this paper, we address the question of how to utilize MIMO for sensing.

This paper considers the problem of designing precoded sensing sequences in a MIMO sensing scenario in the presence of scatterers. The main result of this paper is that unlike the MIMO communications scenario or the MIMO sensing scenario without scatterers, where the optimization of MIMO precoder reduces to an optimization of a fixed transmit covariance, when signal-dependent interferences from scatterers are present, the optimization must be over the MIMO sensing precoding sequence explicitly. This would induce transmit beam patterns that vary across the sensing interval, almost akin to sweeping.

MIMO sensing has attracted significant attention in the recent literature [1]. However, most existing works consider only the targets of interest while neglecting interfering scatterers. In this case, the optimal MIMO precoder design reduces to that of designing a fixed transmit covariance or beam pattern. Examples of such approach include MIMO radar works that design the transmit sample covariance matrix based on various sensing objectives, such as shaping the transmit beampatterns [2], minimizing the Cramér-Rao lower bound (CRLB) [3], and minimizing the Bayesian CRLB (BCRLB) [4], and work in the ISAC context [5] [6] [7] that design beamformer to minimize the sensing CRLB under the communication constraints.

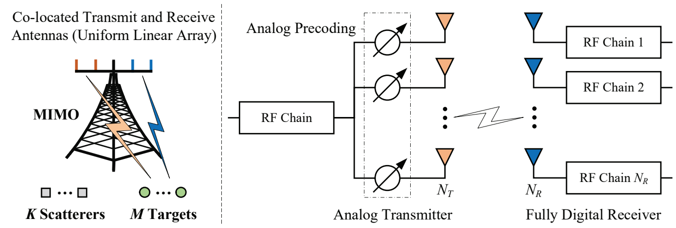

Fig. 1. A monostatic MIMO sensing system with a single-RF-chain transmitter and a fully-digital receiver in the presence of interfering scatterers.

This paper studies a multiple-target MIMO sensing-only system, but with scatterers in addition to the targets of interests, as shown in Fig. 1. We reveal that due to the signal-dependent interference from the reflections of the scatterers, the sensing performance is no longer fully characterized by a single transmit sample covariance matrix, but instead depends on the entire precoding sequence, which should be explicitly designed. We propose an optimization methodology that formulates the problem of minimizing the BCRLB for estimating the target azimuth angles as a max-min fractional program, which can be efficiently solved using a linear transform technique. Furthermore, we show that the optimized precoders should vary across the multiple symbol periods to probe the angular domain of interest, while suppressing interference from the scatterers.

II. System Model

This paper investigates a monostatic MIMO sensing system equipped with co-located N_T transmit antennas and N_R receive antennas. The MIMO sensing scenario consists of M targets of interest and K scatterers. The precoded signals from the transmit antennas are reflected by both the targets and the scatterers. The sensing task is to estimate the azimuth angles of the targets of interest, based on the received echoes. We adopt a Bayesian approach and assume some prior probability distributions on the azimuth angles of the targets and the scatterers, but we do not estimate or track the parameters of the scatterers in order to prevent excessive dimensionality increase in the parameter space. In this scenario, the signals reflected from the scatterers act as interference to the estimation of target angles. Moreover, we also do not estimate or track the path-loss parameters of the targets and the scatterers and assume that they are nuisance random variables with zero-mean and known variances. The goal is to design the sequence of precoded signals across the MIMO arrays and across the sensing interval to optimize the performance of estimating the target angles.

We perform MIMO sensing across N symbol periods. We choose to use the case of analog transmit precoding to illustrate the main points of the paper, but the proposed methodology and the conclusions of the paper equally apply to digital precoding. Here, the receiver is assumed to be fully digital. In this case, the analog precoder over N_T transmit antennas is

$$\mathbf{x} = \mathsf{vec}\Big([\mathbf{x}_1, \mathbf{x}_2, \ldots, \mathbf{x}_N]\Big), \tag{1}$$

where $\mathbf{x}_n \in \mathbb{C}^{N_T \times 1}$ denotes the precoder designed for the n-th symbol period. The entries of $\mathbf{x}$ are subject to the constant-modulus constraint due to the analog constraint, i.e.,

$$|x_n| = 1, \ \ n = 1, 2, \ldots, N_T N. \tag{2}$$

Assuming a uniform linear array configuration for simplicity, the steering vectors for the forward path from the antennas to the target/scatterer at azimuth angle θ, and for the reflected path from the target/scatterer to the antennas, are given by

$$\mathbf{h}_T(\theta) \triangleq \Big[1, e^{j\tau\cos(\theta)}, \ldots, e^{j(N_T-1)\tau\cos(\theta)}\Big]^{\mathsf{T}}, \tag{3}$$

$$\mathbf{h}_R(\theta) \triangleq \Big[1, e^{j\tau\cos(\theta)}, \ldots, e^{j(N_R-1)\tau\cos(\theta)}\Big]^{\mathsf{T}}, \tag{4}$$

where $\tau = 2\pi d/\omega$, ω is the carrier wavelength, and d denotes the spacing between adjacent antennas, typically at $\omega/2$. Then, the round-trip array response is

$$\mathbf{H}(\theta) = \mathbf{h}_R(\theta)\, \mathbf{h}_T^{\mathsf{T}}(\theta)\,. \tag{5}$$

Considering the significant path-loss in high-frequency bands, we only account for the first-order reflections in the received signal model. Moreover, the transmitted symbol is set to 1. This is without loss of generality since any known unit-power symbol can be absorbed into the precoders. Then, the echo signals received across the N_R antennas over the N symbols can be stacked into a single vector $\mathbf{y} \in \mathbb{C}^{N_R N \times 1}$ as

$$\begin{aligned}\mathbf{y} = \mathsf{vec}\Big([\mathbf{y}_1, \mathbf{y}_2, \ldots, \mathbf{y}_N]\Big) &= \sum_{m=1}^{M} \left(\alpha_m \mathbf{I}_N \otimes \mathbf{H}(\theta_m)\right)(\sqrt{p}\mathbf{x}) \\ &+ \sum_{k=1}^{K} \left(\beta_k \mathbf{I}_N \otimes \mathbf{H}(\eta_k)\right)(\sqrt{p}\mathbf{x}) + \mathbf{n} \\ \triangleq \sum_{m=1}^{M} \alpha_m \sqrt{p}\,\mathbf{U}_m \mathbf{x} &+ \sum_{k=1}^{K} \beta_k \sqrt{p}\,\boldsymbol{\Upsilon}_k \mathbf{x} + \mathbf{n},\end{aligned} \tag{6}$$

where θ_m and η_k are the azimuth angles of the m-th target and the k-th interfering scatterer, respectively, and are assumed to be constant over the entire sensing duration; the prior distributions of θ_m and η_k are assumed to be mutually independent and are known a priori. The parameters α_m and β_k denote the path-loss coefficients of the m-th target and the k-th interfering scatterer, respectively; they are modeled as independent random variables distributed as $\mathcal{CN}(0, \varsigma_m^2)$ and $\mathcal{CN}(0, \sigma_k^2)$, respectively [8]. The path-loss coefficients are assumed to remain constant within the sensing duration, and their second-order statistics ς_m^2 and σ_k^2 are known a priori. The per-antenna transmit power is p, and the additive noise $\mathbf{n}$ is distributed as $\mathcal{CN}(\mathbf{0}, \varepsilon^2\mathbf{I})$.

III. Sensing Performance Metric

In this section, we discuss the sensing metric used in this paper and show the effect of interfering scatterers. This paper adopts the BCRLB as the sensing metric. The BCRLB allows the sensing strategy to exploit the prior information of the target and scatterer parameters. It provides a lower bound on the Bayesian mean-squared error of estimators. Specifically, this paper adopts an approach of formulating the BCRLB of the parameters of M targets, while treating the scatterers as interference. These target parameters are $\mathbf{v} \triangleq [\boldsymbol{\theta}^{\mathsf{T}}, \boldsymbol{\alpha}^{\mathsf{T}}]^{\mathsf{T}}$, where

$$\boldsymbol{\theta} \triangleq \Big[\theta_1, \ldots, \theta_M\Big]^{\mathsf{T}}, \tag{7}$$

$$\boldsymbol{\alpha} \triangleq \Big[\mathsf{Re}\{\alpha_1\}, \ldots, \mathsf{Re}\{\alpha_M\}, \mathsf{Im}\{\alpha_1\}, \ldots, \mathsf{Im}\{\alpha_M\}\Big]^{\mathsf{T}}. \tag{8}$$

The BCRLB of $\mathbf{v}$ has the following form:

$$\mathsf{BCRLB}\,(\mathbf{v}) = \mathsf{Tr}\left\{\left(\begin{bmatrix} \boldsymbol{\Phi}_{\mathsf{o}} & \mathbf{C}_{\mathsf{o}} \\ \mathbf{C}_{\mathsf{o}}^{\mathsf{T}} & \mathbf{A}_{\mathsf{o}} \end{bmatrix} + \begin{bmatrix} \boldsymbol{\Phi}_{\mathsf{p}} & \mathbf{C}_{\mathsf{p}} \\ \mathbf{C}_{\mathsf{p}}^{\mathsf{T}} & \mathbf{A}_{\mathsf{p}} \end{bmatrix}\right)^{-1}\right\}, \tag{9}$$

where $\boldsymbol{\Phi}_{\mathsf{o}}$ and $\boldsymbol{\Phi}_{\mathsf{p}}$ are the Bayesian Fisher information matrices (BFIMs) corresponding to $\boldsymbol{\theta}$ from observations and from priors, respectively; $\mathbf{A}_{\mathsf{o}}$ and $\mathbf{A}_{\mathsf{p}}$ denote the BFIMs corresponding to $\boldsymbol{\alpha}$; $\mathbf{C}_{\mathsf{o}}$ and $\mathbf{C}_{\mathsf{p}}$ denote the cross BFIMs between $\boldsymbol{\theta}$ and $\boldsymbol{\alpha}$. The prior BFIMs $\boldsymbol{\Phi}_{\mathsf{p}}$, $\mathbf{A}_{\mathsf{p}}$, and $\mathbf{C}_{\mathsf{p}}$ follow the definition given in [9, Eq. (11)] and are independent of $\mathbf{x}$. Moreover, since the priors are mutually independent, $\boldsymbol{\Phi}_{\mathsf{p}}$ and $\mathbf{A}_{\mathsf{p}}$ are diagonal; $\mathbf{C}_{\mathsf{p}}$ is zero.

The parameters of interest here are the target azimuth angles $\boldsymbol{\theta}$, while the path-loss coefficients $\boldsymbol{\alpha}$ are nuisance parameters. In the proposed methodology, we first include $\boldsymbol{\alpha}$ in the BCRLB, and then extract a lower bound for estimating $\boldsymbol{\theta}$ from the joint BCRLB expression via Schur complement at a later stage. The scatterers are treated as interference; their effect is spatially filtered out based on the difference in the priors of the target angles $\{\theta_m\}_{m=1}^M$ and the scatterers $\{\eta_k\}_{k=1}^K$.

We now show the difference in BCRLB optimization for the scenarios with no scatterers versus the scenarios where signal-dependent interferences from the scatterers are present.

A. Without Interfering Scatterers

In the target-only sensing scenarios, we have

$$\mathbf{y} = \sum_{m=1}^{M} \alpha_m \sqrt{p}\,\mathbf{U}_m \mathbf{x} + \mathbf{n}, \tag{10}$$

where $\mathbf{n}$ has i.i.d. entries across the N symbols. This yields the following expression for the likelihood of $\mathbf{v}$ as a function of the received symbols:

$$\begin{aligned}\ln \mathcal{L}\left(\mathbf{y} \,|\, \mathbf{v}\right) = \sum_{n=1}^{N} \ln \mathcal{L}\left(\mathbf{y}_n \,|\, \mathbf{v}\right) &= -N_R N \ln(\pi\varepsilon^2) \\ &- \sum_{n=1}^{N} \frac{1}{\varepsilon^2} \left\| \mathbf{y}_n - \sum_{m=1}^{M} \alpha_m \sqrt{p}\,\mathbf{H}(\theta_m)\mathbf{x}_n \right\|^2,\end{aligned} \tag{11}$$

where $\mathcal{L}\left(\cdot \,|\, \cdot\right)$ represents the likelihood function. This means the overall Fisher information from the N observations can be expressed as a sum of contributions from each symbol period. We use the BFIM $\mathbf{\Phi}_{\mathsf{o}}$ as an example to illustrate. The (m,m')-th entry of $\mathbf{\Phi}_{\mathsf{o}}$ is given by

$$\begin{aligned}\mathbf{\Phi}_{\mathsf{o}}^{(m,m')} &= -\mathbb{E}_{\mathbf{y},\mathbf{v}}\left[\frac{\partial^2}{\partial\eta_m\partial\eta_{m'}}\ln\mathcal{L}\left(\mathbf{y}|\mathbf{v}\right)\right] \\ &= \frac{2pN}{\varepsilon^2}\cdot \\ &\quad \mathsf{Re}\left\{\mathsf{Tr}\left(\mathbb{E}_{\mathbf{v}}\left[(\alpha_m\dot{\mathbf{H}}(\theta_m))^\dagger(\alpha_{m'}\dot{\mathbf{H}}(\theta_{m'}))\right]\frac{1}{N}\sum_{n=1}^{N}\mathbf{x}_n\mathbf{x}_n^\dagger\right)\right\} \\ &= \frac{2pN}{\varepsilon^2}\,\mathsf{Re}\left\{\mathsf{Tr}\left(\mathbb{E}_{\mathbf{v}}\left[(\alpha_m\dot{\mathbf{H}}(\theta_m))^\dagger(\alpha_{m'}\dot{\mathbf{H}}(\theta_{m'}))\right]\mathbf{R}\right)\right\},\end{aligned} \tag{12}$$

where $\dot{\mathbf{H}}(\theta_m) \triangleq \partial\mathbf{H}(\theta_m)/\partial\theta_m$, and $\mathbf{R} \triangleq \frac{1}{N}\sum_{n=1}^{N}\mathbf{x}_n\mathbf{x}_n^\dagger$. One can observe from (12) that the BFIMs are the functions of $\mathbf{R}$ only. Consequently, designing the precoding sequence amounts to optimizing a single transmit sample covariance $\mathbf{R}$, as done in numerous works in the literature, e.g., [5], [7], [10].

B. With Interfering Scatterers

In the scenario where interfering scatterers are present, the observations are no longer conditionally independent over N given the target parameters, because the interfering scatterers parameters are the same across the N symbols. Furthermore, the exact statistics for the computation of BCRLB is complicated. One way to make the likelihood function and the BCRLB tractable is to model the aggregate interference-plus-noise as a Gaussian random vector with matching mean and covariance matrix. Then, the likelihood of $\mathbf{v}$ given the observations $\mathbf{y}$ can be expressed as in (13) at the bottom of the page, where $\mathbf{\Sigma}(\mathbf{x})$ is the covariance matrix of the aggregate interference-plus-noise and is given by

$$\mathbf{\Sigma}(\mathbf{x}) = \sum_{k=1}^{K} p\sigma_k^2\mathbb{E}_{\eta_k}\Big[\left(\mathbf{\Upsilon}_k\mathbf{x}\right)\left(\mathbf{\Upsilon}_k\mathbf{x}\right)^\dagger\Big] + \varepsilon^2\mathbf{I}_{N_RN}. \tag{14}$$

The (m,m')-th entry of $\mathbf{\Phi}_{\mathsf{o}}$ is

$$\mathbf{\Phi}_{\mathsf{o}}^{(m,m')} = 2p\,\mathsf{Re}\left\{\mathbb{E}_{\mathbf{v}}\left[(\alpha_m\dot{\mathbf{U}}_m\mathbf{x})^\dagger\left(\mathbf{\Sigma}(\mathbf{x})\right)^{-1}\left(\alpha_{m'}\dot{\mathbf{U}}_{m'}\mathbf{x}\right)\right]\right\}, \tag{15}$$

where $\dot{\mathbf{U}}_m \triangleq \partial\mathbf{U}_m/\partial\theta_m$. The key observation is that in contrast to the target-only sensing scenario, the BFIM entries are no longer simple functions of the transmit covariance matrix $\mathbf{R}$. The BCRLB in fact depends explicitly on the sequence of precoders $\{\mathbf{x}_n\}_{n=1}^N$ rather than their second-order sample covariance. Therefore, unlike the target-only case where a time-invariant transmit covariance is sufficient, the precoder design in the presence of interfering scatterers must be over the sequence of $\{\mathbf{x}_n\}_{n=1}^N$ explicitly.

IV. PRECODING FOR MIMO SENSING WITH SCATTERERS

We now propose a design methodology for the precoding sequence $\{\mathbf{x}_n\}_{n=1}^N$ for MIMO sensing with scatterers. Toward this end, we formulate the BCRLB optimization problem for multiple-target angle estimation in this section. Algorithm for solving the problem is presented in the next section.

The first step is to derive the BCRLB for the target angles $\boldsymbol{\theta}$. The BCRLB for estimating $\boldsymbol{\theta}$ is given by the trace of the top-left principal block of the inverse of full BFIM. Using Schur complement, the BCRLB for estimating $\boldsymbol{\theta}$ is given by

$$\begin{aligned}\mathsf{BCRLB}\left(\boldsymbol{\theta}\right) = \mathsf{Tr}\Bigg\{\bigg(&\left(\mathbf{\Phi}_{\mathsf{o}}+\mathbf{\Phi}_{\mathsf{p}}\right) \\ &-\left(\mathbf{C}_{\mathsf{o}}+\mathbf{C}_{\mathsf{p}}\right)\left(\mathbf{A}_{\mathsf{o}}+\mathbf{A}_{\mathsf{p}}\right)^{-1}\left(\mathbf{C}_{\mathsf{o}}+\mathbf{C}_{\mathsf{p}}\right)^{\mathsf{T}}\bigg)^{-1}\Bigg\}.\end{aligned} \tag{16}$$

A key observation allows the above expression to be simplified. Under the assumption that α_m's are independent and follow $\mathcal{CN}\left(0,\varsigma_m^2\right)$, $\mathbf{C}_{\mathsf{o}}$ is zero due to the expectation over $\boldsymbol{\alpha}$. Similarly, the off-diagonal entries of $\mathbf{\Phi}_{\mathsf{o}}$ are also zero. Then, the BCRLB of estimating $\boldsymbol{\theta}$ can be simplified as

$$\mathsf{BCRLB}\left(\boldsymbol{\theta}\right) = \mathsf{Tr}\left\{\left(\mathbf{\Phi}_{\mathsf{o}}+\mathbf{\Phi}_{\mathsf{p}}\right)^{-1}\right\}. \tag{17}$$

Since both $\mathbf{\Phi}_{\mathsf{o}}$ and $\mathbf{\Phi}_{\mathsf{p}}$ are diagonal matrices, the BCRLB for estimating each single target azimuth angle θ_m can now be expressed as

$$\mathsf{BCRLB}\left(\theta_m\right) = \frac{1}{\mathbf{\Phi}_{\mathsf{o}}^{(m,m)}+\mathbf{\Phi}_{\mathsf{p}}^{(m,m)}} \triangleq \frac{1}{\gamma_m(\mathbf{x})}. \tag{18}$$

For the multiple-target azimuth angle estimation problem, we need to decide the relative importance for estimating the different angles. A formulation that ensures fairness is to minimize the maximum BCRLB among all the target angles. Then, the problem of designing precoders to optimize the worst-case BCRLB across all angles can be formulated as

$$\textbf{(P1):}\quad \max_{\mathbf{x}}\ \min_{m}\ \gamma_m(\mathbf{x}) \tag{19a}$$

$$\text{subject to}\ \ |x_n| = 1,\ n = 1,2,\ldots,N_TN. \tag{19b}$$

which is a max-min fractional programming problem with extra constant-modulus constraints.

Before solving problem (P1), one issue that needs to be tackled is that the variable $\mathbf{x}$ is inside the expectations in (14) and (15). These expectations are over the priors of the target and scatterer parameters, which can be explicitly computed using their second-moment matrices. This allows $\mathbf{x}$ to be extracted.

The steps below are similar to those in [11, Theorem 1]. Specifically, define

$$\bar{\mathbf{U}}_m \triangleq \mathbb{E}_{\theta_m}\Big[\mathsf{vec}\left(\dot{\mathbf{U}}_m\right)\mathsf{vec}^\dagger\left(\dot{\mathbf{U}}_m\right)\Big], \tag{20}$$

$$\ln\mathcal{L}\left(\mathbf{y}\,|\,\mathbf{v}\right) = -N_RN\ln(\pi) - \ln|\mathbf{\Sigma}(\mathbf{x})| - \left(\mathbf{y}-\sum_{m=1}^{M}\alpha_m\sqrt{p}\,\mathbf{U}_m\mathbf{x}\right)^\dagger\left(\mathbf{\Sigma}(\mathbf{x})\right)^{-1}\left(\mathbf{y}-\sum_{m=1}^{M}\alpha_m\sqrt{p}\,\mathbf{U}_m\mathbf{x}\right) \tag{13}$$

and let its rank be T_m. Let $w_m^{[i]}$ and $\mathbf{u}_m^{[i]}$ be the i-th eigenvalue and the corresponding eigenvector of $\bar{\mathbf{U}}_m$. Then, $\mathbf{\Phi}_{\mathsf{o}}^{(m,m)}$ can be rewritten as

$$\mathbf{\Phi}_{\mathsf{o}}^{(m,m)} = 2p\varsigma_m^2 \sum_{i=1}^{T_m} w_m^{[i]} \left(\dot{\mathbf{U}}_m^{[i]}\mathbf{x}\right)^\dagger (\mathbf{\Sigma}(\mathbf{x}))^{-1} \left(\dot{\mathbf{U}}_m^{[i]}\mathbf{x}\right), \quad (21)$$

where, with a slight abuse of notation, $\dot{\mathbf{U}}_m^{[i]}$ represents the matrix reshaped from $\mathbf{u}_m^{[i]}$, i.e., $\dot{\mathbf{U}}_m^{[i]} \triangleq \mathsf{vec}^{-1}(\mathbf{u}_m^{[i]})$.

Similarly, to rewrite the covariance matrix $\mathbf{\Sigma}(\mathbf{x})$, we define

$$\bar{\mathbf{\Upsilon}}_k \triangleq \mathbb{E}_{\eta_k}\Big[\mathsf{vec}\left(\mathbf{\Upsilon}_k\right) \mathsf{vec}^\dagger\left(\mathbf{\Upsilon}_k\right)\Big], \quad (22)$$

and let its rank be R_k. Let $\kappa_k^{[i]}$ and $\boldsymbol{\upsilon}_k^{[i]}$ be the i-th eigenvalue and the corresponding eigenvector of $\bar{\mathbf{\Upsilon}}_k$. Then, $\mathbf{\Sigma}(\mathbf{x})$ can be rewritten as

$$\mathbf{\Sigma}(\mathbf{x}) = \sum_{k=1}^{K}\sum_{i=1}^{R_k} p\sigma_k^2 \kappa_k^{[i]} \left(\mathbf{\Upsilon}_k^{[i]}\mathbf{x}\right)\left(\mathbf{\Upsilon}_k^{[i]}\mathbf{x}\right)^\dagger + \varepsilon^2 \mathbf{I}_{N_R N}, \quad (23)$$

where $\mathbf{\Upsilon}_k^{[i]} \triangleq \mathsf{vec}^{-1}(\boldsymbol{\upsilon}_k^{[i]})$. In this way, the precoding sequence design problem (P1) now only involves deterministic quantities.

V. Algorithm for Optimizing the Precoders

To tackle the max-min fractional programming problem (P1) in an efficient manner, we employ a linear transform technique, which can transform a ratio function over a constant-modulus variable into a linear function, to handle the multiple objectives. This technique was originally proposed in our prior work [11] to maximize a fractional objective for reconfigurable intelligent surface (RIS)-assisted ISAC systems and was extended into the max-min-ratio case for RIS-assisted wireless communication systems in [12]. In this paper, we adopt it to solve (P1).

A. Constant-Modulus Linear Transform

To state the linear transform technique, we begin by defining the following general form of the fractional function:

$$f(\mathbf{x}) \triangleq (\mathbf{A}\mathbf{x})^\dagger (\mathbf{D}(\mathbf{x}))^{-1} (\mathbf{A}\mathbf{x}), \quad (24)$$

where the variable $\mathbf{x}$ is an $\bar{N}$-dimensional complex vector with each entry being constant-modulus; the denominator matrix $\mathbf{D}(\mathbf{x})$ is $\bar{M}$-dimensional and is defined as

$$\mathbf{D}(\mathbf{x}) \triangleq \sum_k \mu_k (\mathbf{B}_k\mathbf{x})(\mathbf{B}_k\mathbf{x})^\dagger + \mathbf{C}. \quad (25)$$

The matrix $\mathbf{C}$ is positive definite, and μ_k is positive for all k. The linear transform for $f(\mathbf{x})$ is stated in the following lemma.

Lemma 1 ([11, Lemma 2]): A lower bound for the fractional function $f(\mathbf{x})$ is

$$f(\mathbf{x}) \geq \bar{f}(\mathbf{x},\mathbf{z},\boldsymbol{\lambda}) \triangleq 2\,\mathsf{Re}\left\{\mathbf{x}^\dagger \mathbf{u}(\mathbf{z},\boldsymbol{\lambda})\right\} + c(\mathbf{z},\boldsymbol{\lambda}), \quad (26)$$

for all $\boldsymbol{\lambda} \in \mathbb{C}^{\bar{M}}$, and $\mathbf{x},\mathbf{z} \in \mathbb{S}^{\bar{N}}$, where $\mathbb{S} \triangleq \{x \in \mathbb{C} \,|\, |x| = 1\}$. The linear coefficient of $\mathbf{x}$ in (26) is given by

$$\mathbf{u}(\mathbf{z},\boldsymbol{\lambda}) = (\delta\mathbf{I} - \mathbf{M})\mathbf{z} + \mathbf{A}^\dagger\boldsymbol{\lambda}, \quad (27)$$

where the matrix $\mathbf{M}$ is given by

$$\mathbf{M} = \sum_k \mu_k \left(\mathbf{B}_k^\dagger\boldsymbol{\lambda}\right)\left(\mathbf{B}_k^\dagger\boldsymbol{\lambda}\right)^\dagger, \quad (28)$$

the parameter δ is the trace of $\mathbf{M}$, and $c(\mathbf{z},\boldsymbol{\lambda})$ is given by

$$c(\mathbf{z},\boldsymbol{\lambda}) = \mathbf{z}^\dagger\mathbf{M}\mathbf{z} - 2\delta\bar{N} - \boldsymbol{\lambda}^\dagger\mathbf{C}\boldsymbol{\lambda}. \quad (29)$$

The equality in (26) is achieved at

$$\mathbf{z}^\star = \mathbf{x}, \text{ and } \boldsymbol{\lambda}^\star = (\mathbf{D}(\mathbf{x}))^{-1}\mathbf{A}\mathbf{x}. \quad (30)$$

Lemma 1 directly provides an equivalent reformulation of a max-min-ratio problem in the following corollary.

Corollary 1: The max-min fractional program with constant-modulus constraints,

$$\max_{\mathbf{x}} \ \min_{m} \ \xi_m f_m(\mathbf{x}) \quad (31a)$$
$$\text{subject to } \ |x_n| = 1, \ \forall n, \quad (31b)$$

where $\xi_m > 0$, $\forall m$, is equivalent to

$$\max_{\mathbf{x},\mathbf{z},\boldsymbol{\lambda}_m} \ \min_{m} \ \xi_m \bar{f}_m(\mathbf{x},\mathbf{z},\boldsymbol{\lambda}_m) \quad (32a)$$
$$\text{subject to } \ |x_n| = |z_n| = 1, \ \forall n. \quad (32b)$$

B. Solving Problem (P1)

By applying Corollary 1, problem (P1) can be equivalently transformed into the following problem:

$$\textbf{(P2):} \quad \max_{\mathbf{x},\mathbf{z},\mathbf{\Lambda}_m} \ \min_{m} \ \bar{\gamma}_m(\mathbf{x},\mathbf{z},\mathbf{\Lambda}_m) \quad (33a)$$
$$\text{subject to } \ |x_n| = |z_n| = 1, \ \forall n. \quad (33b)$$

The new transformed objective function $\bar{\gamma}_m(\mathbf{x},\mathbf{z},\mathbf{\Lambda}_m)$ is

$$\bar{\gamma}_m(\mathbf{x},\mathbf{z},\mathbf{\Lambda}_m) = 4p\varsigma_m^2\,\mathsf{Re}\left\{\mathbf{x}^\dagger\mathbf{u}_m(\mathbf{z},\mathbf{\Lambda}_m)\right\} + 2p\varsigma_m^2 c_m(\mathbf{z},\mathbf{\Lambda}_m) + \mathbf{\Phi}_{\mathsf{p}}^{(m,m)}, \quad (34)$$

where $\mathbf{\Lambda}_m$ refers to $[\boldsymbol{\lambda}_m^{[1]},\ldots,\boldsymbol{\lambda}_m^{[T_m]}]$, the linear coefficient of $\mathbf{x}$ in (34) is given by

$$\mathbf{u}_m(\mathbf{z},\mathbf{\Lambda}_m) = \sum_{i=1}^{T_m} w_m^{[i]}\left(\left(\delta_m^{[i]}\mathbf{I} - \mathbf{M}_m^{[i]}\right)\mathbf{z} + \left(\dot{\mathbf{U}}_m^{[i]}\right)^\dagger\boldsymbol{\lambda}_m^{[i]}\right), \quad (35)$$

the matrix $\mathbf{M}_m^{[i]}$ is given by

$$\mathbf{M}_m^{[i]} = \sum_{k=1}^{K}\sum_{r=1}^{R_k} p\sigma_k^2\kappa_k^{[r]}\left(\left(\boldsymbol{\lambda}_m^{[i]}\right)^\dagger\mathbf{\Upsilon}_k^{[r]}\right)^\dagger\left(\left(\boldsymbol{\lambda}_m^{[i]}\right)^\dagger\mathbf{\Upsilon}_k^{[r]}\right), \quad (36)$$

the parameter $\delta_m^{[i]}$ denotes the trace of the positive semi-definite matrix $\mathbf{M}_m^{[i]}$, and $c_m(\mathbf{z},\mathbf{\Lambda}_m)$ is given by

$$c_m(\mathbf{z},\mathbf{\Lambda}_m) = \sum_{i=1}^{T_m} w_m^{[i]}\left(\mathbf{z}^\dagger\mathbf{M}_m^{[i]}\mathbf{z} - 2\delta_m^{[i]}N_T N - \varepsilon^2\left\|\boldsymbol{\lambda}_m^{[i]}\right\|_2^2\right). \quad (37)$$

We now solve problem (P2) in an iterative manner. When $\mathbf{x}$ is fixed, the optimal $\mathbf{z}^\star$ and $(\boldsymbol{\lambda}_m^{[i]})^\star$ are given by

$$\mathbf{z}^\star = \mathbf{x}, \text{ and } (\boldsymbol{\lambda}_m^{[i]})^\star = (\mathbf{\Sigma}(\mathbf{x}))^{-1}\dot{\mathbf{U}}_m^{[i]}\mathbf{x}. \quad (38)$$

When $\mathbf{z}$ and $\boldsymbol{\lambda}_m^{[i]}$ are fixed, the optimal $\mathbf{x}^\star$ is given by [12]

$$\mathbf{x}^\star(\boldsymbol{\nu}^\star) = \exp\left(j \arg\left(\boldsymbol{\pi}(\boldsymbol{\nu}^\star) \triangleq \sum_{m=1}^{M} \nu_m^\star \varsigma_m^2 \mathbf{u}_m(\mathbf{z}, \boldsymbol{\Lambda}_m) \right)\right), \tag{39}$$

provided that $[\boldsymbol{\pi}(\boldsymbol{\nu}^\star)]_n \neq 0$, $\forall n$. Here, $\boldsymbol{\nu}^\star$ denotes the optimal solution of the following convex problem:

$$\textbf{(P3):} \quad \underset{\boldsymbol{\nu} \in \Delta^{M-1}}{\text{minimize}} \; \sum_{m=1}^{M} \nu_m \bar{\gamma}_m(\mathbf{x}^\star(\boldsymbol{\nu}), \mathbf{z}, \boldsymbol{\Lambda}_m), \tag{40}$$

where Δ^{M-1} denotes the standard simplex in $\mathbb{R}^M$. Empirically, for the scenario considered in this paper, where the dimension of $\mathbf{x}$ is much greater than the number of targets, the condition $[\boldsymbol{\pi}(\boldsymbol{\nu}^\star)]_n \neq 0$, $\forall n$, is almost always satisfied.

VI. Numerical Results

In this section, we present simulation results. The simulation environment is set as follows.

- The normalized transmit power $p\varsigma_m^2/\varepsilon^2$ is set as -10 dB. The normalized interference power $p\sigma_k^2/\varepsilon^2$ is set as 20 dB.
- The numbers of the transmit and receive antennas are set as $N_T = 8$ and $N_R = 4$, respectively. The spacing between two adjacent antennas is set as half a wavelength.
- Sensing takes place over $N = 10$ symbol periods.

We use beam patterns to illustrate the solutions. The transmit beam pattern of the precoder for the n-th period is defined as

$$\mathcal{S}_n(\theta) \triangleq \left| \mathbf{h}_T^\top(\theta)\, \mathbf{x}_n \right|^2, \;\; \forall n \in [1, N]. \tag{41}$$

Note that the transmit beam pattern alone does not explicitly show the system's capability of suppressing the interference. To verify whether a sequence of precoders can generate nulls aligned with the directions of interfering scatterers, we define the overall beam pattern for the entire system as

$$\mathcal{Q}(\theta) = \left| \mathbf{f}^\dagger \left(\mathbf{I}_N \otimes \mathbf{H}(\theta) \right) \mathbf{x} \right|^2, \tag{42}$$

where $\mathbf{f}$ is the LMMSE combiners.

We present the transmit and overall beam patterns in Fig. 2. In this figure, two targets are uniformly distributed over $[30°, 70°]$ and $[90°, 130°]$, respectively, while two interfering scatterers are uniformly distributed over $[140°, 180°]$. The first row shows the beam patterns of the proposed solution of optimizing $N = 10$ precoders. The resulting transmit beams exhibit a sweep-like pattern, which, under the limited degrees of freedom of analog precoding, not only enables effective coverage of the region of interest but also facilitates the formation of nulls to better mitigate interference, as shown in the overall beam pattern. The second row shows the beam patterns of strategy of fixed transmit sample covariance $\mathbf{R}$, i.e., designing a single-symbol precoder to be used across all $N = 10$ symbol periods. The resulting beam pattern achieves limited interference suppression because of its static precoding structure. Moreover, compared with the proposed precoding sequence design, it suffers from insufficient coverage of the entire target region. The last row shows the beam patterns of a target-only strategy, i.e., designing

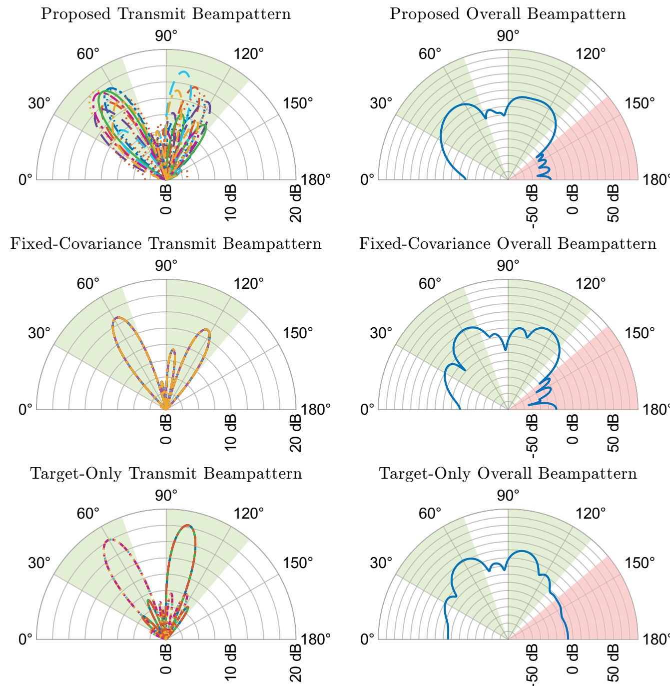

Fig. 2. Transmit beam patterns and overall beam patterns of different precoding strategies. Top: Proposed precoding sequence design; Middle: Fixed transmit sample covariance; Bottom: Target-only without accounting for scatterers.

TABLE I
Bayesian Cramér-Rao lower bound (BCRLB) $[\text{deg}^2]$ of different precoding sequence design strategies.

Number of Symbols	Proposed	Fixed Covariance	Target-Only
$N = 1$	<u>1.4283</u>	<u>1.4283</u>	3.3915
$N = 4$	<u>0.3671</u>	0.4185	0.7171
$N = 10$	<u>0.1488</u>	0.1761	0.3259

$N = 10$ precoders by only focusing on the target regions while neglecting the interfering scatterers. In this strategy, despite optimizing a sequence of precoders, all precoders result in identical beam patterns. Moreover, the resulting solution has no nulls for interference. The results in Table I further validate the superior performance of the proposed precoding solution.

VII. Conclusion

This paper proposes a methodology for designing a sequence of analog precoders for multi-target MIMO sensing in the presence of interfering scatterers. The BCRLB optimization problem is formulated as a max-min fractional program with constant-modulus constraints and can be efficiently solved by using a linear transform technique. This paper reveals that, in the presence of interfering scatterers, effective MIMO sensing requires designing the entire precoding sequence across multiple symbol periods, as the sensing performance depends on the entire precoding sequence, rather than a fixed transmit sample covariance, to cover the target directions and to suppress the signal-dependent interference from the scatterers.

References

[1] F. Liu, Y. Cui, C. Masouros, J. Xu, T. X. Han, Y. C. Eldar, and S. Buzzi, "Integrated sensing and communications: Toward dual-functional wireless networks for 6G and beyond," *IEEE J. Sel. Areas Commun.*, vol. 40, no. 6, pp. 1728–1767, Jun. 2022.

[2] P. Stoica, J. Li, and Y. Xie, "On probing signal design for MIMO radar," *IEEE Trans. Signal Process.*, vol. 55, no. 8, pp. 4151–4161, Aug. 2007.

[3] J. Li, L. Xu, P. Stoica, K. W. Forsythe, and D. W. Bliss, "Range compression and waveform optimization for MIMO radar: A CramÉr–Rao bound based study," *IEEE Trans. Signal Process.*, vol. 56, no. 1, pp. 218–232, Jan. 2008.

[4] J. Yao and S. Zhang, "Optimal transmit signal design for multi-target MIMO sensing exploiting prior information," in *IEEE Global Commun. Conf. (GLOBECOM)*, Cape Town, South Africa, Dec. 2024.

[5] F. Liu, Y.-F. Liu, A. Li, C. Masouros, and Y. C. Eldar, "Cramér-rao bound optimization for joint radar-communication beamforming," *IEEE Trans. Signal Process.*, vol. 70, pp. 240–253, 2022.

[6] K. M. Attiah and W. Yu, "Uplink-downlink duality for beamforming in integrated sensing and communications," *accepted in IEEE J. Sel. Areas Inf. Theory*, 2026. [Online]. Available: https://arxiv.org/abs/2509.13661

[7] Y. Xiong, F. Liu, Y. Cui, W. Yuan, T. X. Han, and G. Caire, "On the fundamental tradeoff of integrated sensing and communications under Gaussian channels," *IEEE Trans. Inf. Theory*, vol. 69, no. 9, pp. 5723–5751, Sep. 2023.

[8] A. Alkhateeb, O. El Ayach, G. Leus, and R. W. Heath, "Channel estimation and hybrid precoding for millimeter wave cellular systems," *IEEE J. Sel. Topics Signal Process.*, vol. 8, no. 5, pp. 831–846, Oct. 2014.

[9] C. Xu and S. Zhang, "MIMO integrated sensing and communication exploiting prior information," *IEEE J. Sel. Areas Commun.*, vol. 42, no. 9, pp. 2306–2321, Sep. 2024.

[10] F. Liu, L. Zhou, C. Masouros, A. Li, W. Luo, and A. Petropulu, "Toward dual-functional radar-communication systems: Optimal waveform design," *IEEE Trans. Signal Process.*, vol. 66, no. 16, pp. 4264–4279, Aug. 2018.

[11] Y. Liu, K. M. Attiah, and W. Yu, "RIS-assisted joint sensing and communications via fractionally constrained fractional programming," *IEEE Trans. Wireless Commun.*, vol. 25, pp. 1674–1689, 2026.

[12] Y. Liu and W. Yu, "Constant-modulus linear transform for RIS beamforming in uplink multiuser MIMO systems," in *IEEE Int. Conf. Acoust., Speech Signal Process. (ICASSP)*, Barcelona, Spain, May 2026.